ADVANCED MATERIALS
www.advmat.de

Materials Views
www.MaterialsViews.com

Flexible, Transparent Contacts for Inorganic Nanostructures and Thin Films

*Daniel B. Turner-Evans, Hal Emmer, Christopher T. Chen, and Harry A. Atwater**

Silver nanowire (Ag nw) contacts have attracted the attention of the material science community for their high transmission and low resistivity (≈80% across the visible spectrum with a sheet resistance of ≈20 Ω/□), flexibility, and ease of processing.[1–3] While a number of organic solar cells and organic light emitting diodes have incorporated Ag nw contacts,[4–8] their application to inorganic devices has been far more limited.[3,9,10] Instead, thin film and nanostructured inorganic films rely on brittle conductive oxide contacts, limiting the devices to inflexible architectures. Here, we report an approach that uses Ag nws with inorganic semiconductors by depositing metal nanoparticles on the semiconductor surface to create localized contacts. The Ag nws can then form a continuous top contact by bonding to the metal nanoparticle layer. In particular, we combine electroless nickel deposition with dropcast Ag nws to create flexible, transparent contacts to polymer embedded, photovoltaic silicon (Si) microwires (**Figure 1**). With this scheme, we demonstrate a monolithic array of 100 000 s of single wire solar cells connected in parallel with an overall series resistance of 14.0 Ω cm^2, a fill factor of 55.5%, and a Si wire contact yield of >99%.

Micro- and nanowire solar cells are an emerging inorganic photovoltaic technology that requires a flexible, transparent top contact.[11–17] Arrays of Si wires absorb up to 85% of incident sunlight,[18] and single wire devices have demonstrated open circuit voltages of ≈600 mV and the potential for greater than 17% efficient large area devices.[19] Contacts to Si microwire solar cells were therefore chosen as a model platform, although metal nanoparticle/Ag nw contacting schemes should be broadly applicable to a variety of inorganic films and structures.

Si wire arrays were grown p-type ($N_A \approx 1 \times 10^{17}$ as determined by 4 point conductivity measurements on individual wires) through high temperature, atmospheric pressure chemical-vapor-deposition. The wires were cleaned, masked with a SiO_x barrier, and diffusion doped to create an n-type emitter, as described previously.[19] Next, the method of Plass et al. was modified to embed the wire array in silicone polymer (Dow Corning 93-500 Space Grade Encapsulant), leaving ≈5 μm of the wire tips exposed for contacting (see the Supporting Information for more details).[20] While Plass et al. used poly(dimethlysiloxane) (PDMS) to infill the wires, PDMS was found to repel the electroless Ni solution and hence the use of 93–500, which was found to tolerate the Ni solution and was otherwise functionally equivalent to the PDMS.

Ohmic nickel nanoparticle (Ni np) contacts were formed on the Si wires by immersing the Si in an aqueous solution of nickel chloride, sodium hypophosphite, and sodium succinate (Nickelex, Transene, Inc). The hypophosphite is oxidized at the semiconductor surface, allowing the Ni^{2+} ions to scavenge the resulting electrons and to nucleate on the semiconductor. The temperature of the solution and the deposition time were varied in order to optimize the Ni np coverage. At 80 °C, the oxidation occurred selectively at the wire edges, as seen in Figure 1. The edge sites likely catalyze the oxidation reaction. By limiting the deposition time to 30 sec under these conditions, Ni nps could be made to line the edges of the wires without obstructing the wire tops or sidewalls, an important advantage for coupling light into the Si wire solar cells. Longer deposition times (>1 min) led to full, opaque coverage on the wire sidewalls, and devices made from these wires had a series resistance of 1.38 ± 0.03 Ω cm^2. This resistance was measured by contacting 3–5 wires with a nanoprobe and by then forward biasing the contacted devices until the current–voltage relationship was linear, at around 1 V (see Supporting Information for further details).

Immediately after plating Ni nps onto the wires, Ag nws (Cambrios ClearOhm) were drop-cast onto the embedded array to form an interconnected top contact. Xu and Zhu demonstrated conductive and stretchable Ag nw networks by embedding the Ag nws in the top layer of a film of PDMS, and our approach is thus analogous to their technique.[2] As seen in Figure 1b, the Ag nws wrap around the Si wires, forming good mechanical contact to the Ni nps. Optical properties of the silicone polymer on glass and Ag nws on polymer on glass can be seen in **Figure 2**a. Transmission and reflection values were obtained with integrating sphere measurements,[18] and the remainder of the light was assumed to be absorbed. The Ag nws absorb mildly in the blue (<10% at 400 nm) near their plasmon resonance,[21] but otherwise transmit broadly across the spectrum. Reflection losses come from the polymer/air/glass index contrasts. The Ag nw dispersion on polymer on glass had a sheet resistance of 10 Ω/□, as measured with a 4 pt probe.

The optical properties of polymer embedded Si wire arrays with and without the Ni np and Ag nw contact layer are contained in Figure 2b. These arrays were removed from the Si wafer growth substrate by mechanical force with a razor blade,

D. B. Turner-Evans, H. Emmer, C. T. Chen, Prof. H. A. Atwater
T. J. Watson Laboratories of Applied Physics
California Institute of Technology
Pasadena, CA 91125, USA
E-mail: haa@caltech.edu

DOI: 10.1002/adma.201300927

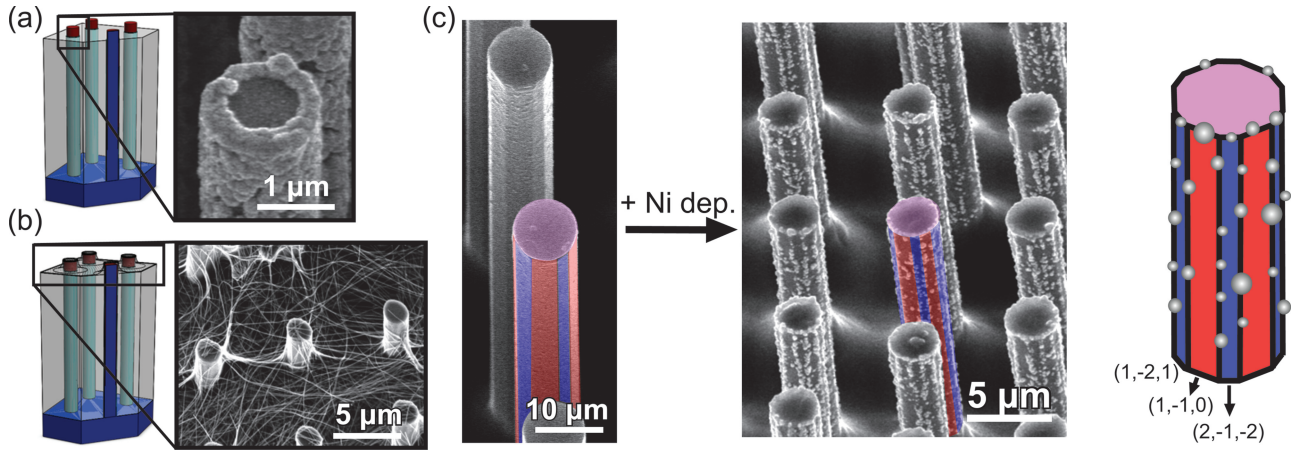

Figure 1. Overview of the two stage top contacting scheme. a) Ni nanoparticles are deposited on the Si wires through electroless deposition. b) Ag nanowires are drop-cast on the array to create a continuous top contact. c) By varying the deposition time and temperature, the Ni nps can be limited to coat the wire edges alone: (left) SEM of the array before and after Ni np deposition; (right) schematic of the wire crystal morphology and Ni np sites.

leaving freestanding polymer/wire films. The films were placed on a glass coverslip to keep them flat during integrating sphere measurement. While the measured absorption of the Si wire/Ni np/Ag nw structures is a convolution of absorption from all three of the materials, the absorption profile looks identical to the profile of the Si wires alone, suggesting that the Ag and Ni do not have a large impact on the overall device behavior. The absorption falls by ≈10% across the spectrum due to reflection losses introduced by the Ni nps and Ag nws. The Ag nw films are denser on the Si arrays than on the planar polymer coated substrate due to their 3D morphology, leading to higher reflection losses.

In parallel to optical measurements, the current–voltage behavior of wires still on the Si substrate was measured. The wires at the substrate edge were mechanically removed to minimize shunting to the substrate through Ag nws at the edges, and Ga/In was scratched into the wafer to form a back contact. The electrical characteristics of an exemplary sample are shown in **Figure 3**. For the purpose of calculating the current density and the series resistance, light-beam induced current (LBIC) maps of the device were fed into image analysis software (ImageJ) to set the active area perimeter and calculate the area. Internal inactive areas (e.g., the small dark spots seen in Figure 3b) were included in the total area. The lower right corner of the device is not contacted as the dropcast polymer completely covers the Si wires in that region. The characteristics of the device are outlined in **Table 1**. The series resistance (R_{Series}) was calculated from the slope at open circuit voltage (V_{OC}) and and the shunt resistance (R_{Shunt}) was calculated from the slope at short circuit (J_{SC}). Though the overall conversion efficiency is low, at 2.8%, the V_{OC} and J_{SC} can be improved by adding surface passivation and Al_2O_3 scattering particles to the wires, as described elsewhere.[12,19] In contrast, the fill factor (55.5%) and series resistance (14.0 Ω cm^2) are direct results of the Ni np/Ag nw contacting scheme. The series resistance is likely dominated by the Ni np/Si wire contact. Whereas this resistance was found to be 1.38 Ω cm^2 for wires fully coated with Ni, the measured device has ≈10 times fewer Ni nanoparticles, leading to the higher resistance. In contrast, the Ag nws contribute at most ≈1 Ω cm^2 to the overall series resistance (10 Ω/□ over ≈0.1 cm^2) and the resistance due to transport through the emitter (doped ≈ 1×10^{19} cm^{-3}) and base are negligible.[19] The Ag nw/Ni np contact may also be a bottleneck. Optimization of the Ni nanoparticle coverage or annealing the devices may lower the sheet resistance and increase the fill factor.

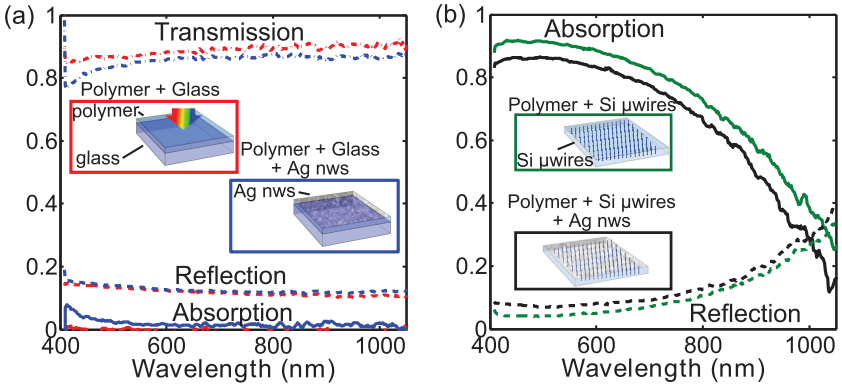

Figure 2. Optical properties of device components. a) Transmission, reflection, and absorption for silicone polymer coated glass slides and Ag nw-coated polymer-covered glass slides. b) Transmission and reflection for polymer embedded Si wire arrays and Ni np and Ag nw-contacted polymer embedded arrays.

The incident photon to conversion efficiency (IPCE) curve of Figure 3c has a similar shape to the absorption profiles of Figure 2b, suggesting that most of the aforementioned absorption can, in fact, be attributed to the Si wires. The difference between the IPCE and absorption curves is likely due to the finite diffusion length within the wires which will lead to recombination losses rather than current collection. Additionally, the substrate (not present in the integrating sphere measurements), will absorb some of the light, though it is degenerately doped and

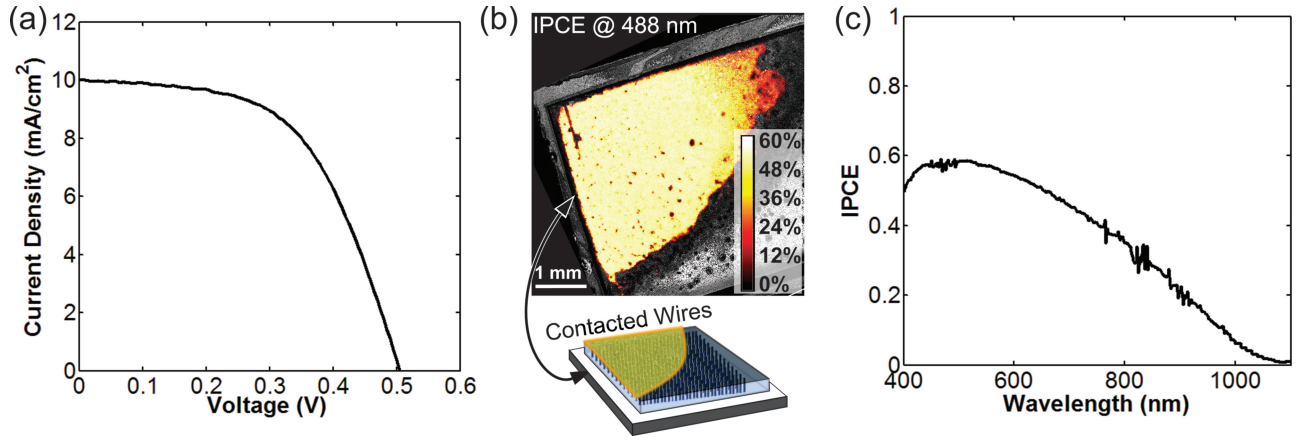

Figure 3. Electronic properties of an on substrate Ni np/Ag nw embedded Si wire array solar cell. a) AM 1.5G current–voltage curve. b) Incident photon to current efficiency (IPCE) profile map at 488 nm showing the extent of carrier collection. The IPCE map is overlaid on a reflected confocal image. The cartoon demonstrates the contacted area of the device. The Si wires in the lower right corner of the device are completely covered with polymer and hence are not contacted. c) IPCE across the AM1.5G spectrum.

Table 1. AM1.5G electrical characteristics of an on substrate Ni np/Ag nw contacted, Si wire array solar cell.

Cell	Area [cm^2]	J_{SC} [mA cm^{-2}]	V_{OC} [V]	Fill Factor [%]	Efficiency [%]	R_{Shunt} [Ω cm^2]	R_{Series} [Ω cm^2]
On Substrate (Figure 3)	0.103	10.0	0.505	55.5	2.80	445	14.0

thus will not appreciably contribute to the IPCE as any generated carriers will rapidly recombine.[12] Also of note, despite the evident scratch on the upper left hand corner of the sample in Figure 3b, the shunt resistance is large and the rest of the device collects photocurrent uniformly. In contacting 100 000s of Si nanowires all in parallel, the loss of individual devices does not substantially decrease the overall device performance, in contrast to a defective area in a monolithic cell.

To compare the Ni np/Ag nw contacting scheme to a more conventional contact for thin film solar cells, 20 nm of indium tin oxide (ITO) ($\rho \approx 7 \times 10^{-4}$ Ω cm) were sputtered onto an infilled wire array. The ITO readily fractured in the polymer infilled area between Si wires and hence Ag nws were spun onto the ITO coated array in order to make contacts over large areas, with the ITO serving to make localized contact to the Si. The cell had comparable performance to the device in Figure 3 (see Supporting Information, Table S1, Figure S4), with an efficiency of 2.51%, a fill factor of 54.6%, and a series resistance of 9.27 Ω cm^{-2}. However, in some regions the Ag nws fractured along with the ITO, leading to inactive areas, and thus the ITO based contact proved to be less robust than the Ni np scheme and hence was not pursued further.

Finally, polymer embedded, Ni np/Ag nw contacted Si wire arrays were peeled off of the growth substrate with a razor blade and Au was evaporated on the back to make a free standing, flexible device. A Ag busbar was also added to aid in making contact with an electrical probe. **Figure 4** shows LBIC maps and current–voltage curves of the device on and off of the growth substrate. The photoresponse of individual wires can be made out in the magnified region. The ratio of individual wires contacted (as evidenced by a ≈3 µm diameter bright spot in the LBIC map) to the total number of wires in the device (1 per 7 × 7 µm area) yielded a >99% contact yield. The wire array electrical performance was measured both on substrate and after peel-off, and the performance per contacted area is virtually identical before and after. However, the electrical properties are inferior to the device shown in Figure 3 due to the lower quality of the Si wire arrays used for this sample. The "peeled off" curve in Figure 4 was measured by flattening the wire array; it naturally rolled into a cylinder with a ≈1 mm diameter due to strain built up during

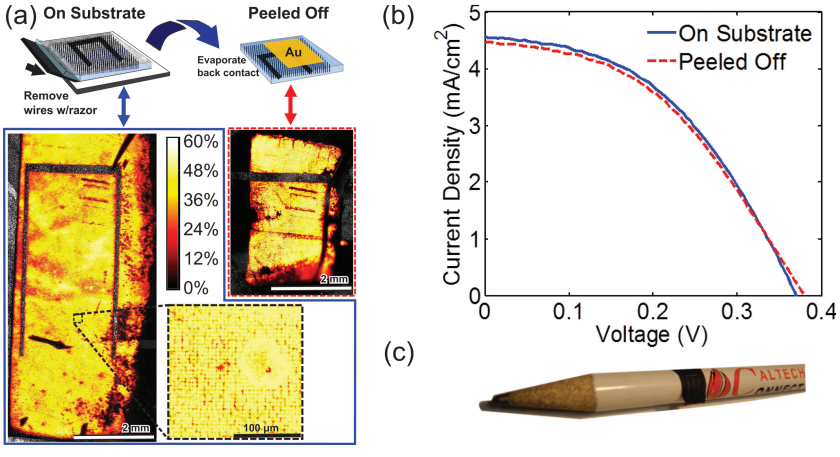

Figure 4. Performance of a peeled off wire array. a) (above) Diagram showing the peel off and back contacting of wire arrays embedded in polymer. (below) IPCE map at 488 nm for a cell on and off the substrate showing the high contact yield both before and after the peel off step. b) AM 1.5G current–voltage curve for the cell on substrate and peeled off. c) Peeled off cell wrapped around a pencil demonstrating the device flexibility.

the polymer curing process. Figure 4c shows the cell wrapped around a pencil with radius of 3.61 mm. Attempts to clamp the end of the peeled off film in order to controllably alter the radius of curvature resulted in the film tearing; the ≈100 μm thick films yielded under the shear stress. Further encapsulation of the arrays will be needed to measure the performance as a function of radius of curvature and number of cycles of rolling and unrolling.[17]

In conclusion, we have demonstrated a two step contacting process that allows flexible, transparent Ag nw contacts to be used with inorganic materials. We demonstrate flexible Si wire array solar cells with conversion efficiencies of up to 2.80%, fill factors of up to 55.5%, and series resistances of 14.0 Ω cm^2. Though n-Si was contacted through this scheme, Ni is also an ohmic contact for p-Ge, p-Si, n-InGaAs, p-InGaAs, n-InP, n-InSb, and p-SiC, making this technique broadly applicable to a variety of other inorganic semiconductors.[22] A number of other metals can also be readily deposited via electroless deposition, further expanding the range of accessible materials. Finally, selected deposition along crystal edges, as seen with the Ni nps, should be possible with other micro- or nanostructured semiconductors. Overall, this contacting paradigm should be broadly applicable to a wide array of inorganic device geometries.

Experimental Section

Si p-n Junction Wire Array Fabrication: A degenerately doped, p-type, Si <111> wafer with 500 nm of oxide was selectively photolithographically patterned, etched, and coated with 400 nm of Cu to form a hexagonal array of Cu catalyst particles in contact with the Si substrate. $SiCl_4$ chemical vapor deposition was then used with BCl_3 to grow large area, p-type, uniform arrays of single crystalline Si wires through the vapor-liquid-solid growth process. After growth, the wires were cleaned with RCA1 and RCA2 and a 30 s KOH etch before a 200 nm dry thermal oxide was grown on the surface. A solution of 10:1:50 w/w/w PDMS base:PDMS curing agent:toluene was then spun into the wire array at 3000 rpm for 30 s and then baked at 60 °C for 20 min to protect the bottom 20 μm of the oxide from a subsequent buffered hydrofluoric acid (BHF) etch which exposed the upper portion of the underlying Si wires for doping. The PDMS was then removed with 1:1 dimethylformamide:tetra butyl ammonium formamide in water, and the arrays were cleaned with piranha and RCA-2. A solid source doping (CeP_5O_{14}) furnace was used to dope the exposed Si, creating an n-type emitter and resulting in a radial wire array solar cell.[19] Finally, a 10:1:15 w/w/w ratio of Dow Corning 93-500 Space Grade Encapsulant base, 93-500 Space Grade Encapsulant curing agent, and toluene was mixed to create a dilute film that was drop cast on the wires at 3000 rpm for 30 s multiple times until the wires were completely covered with polymer. The surface was then completely covered with toluene which was rapidly spun off at 3000 rpm to leave ≈5 μm of the tips exposed. The film was cured at 60 °C for 10 h.

Top-Contact Formation: The silicone polymer embedded wire array was placed in 1:1 dimethylformamide:tetra butyl ammonium formamide in water for 30 s to clean the polymer off of the wire tips and then immersed in BHF for 5 min to remove the dopant oxide from the emitter formation. The array was submerged in a 80 °C electroless Ni solution (Nickelex, Transene, Inc.) for 30 s then immediately covered with an aqueous solution of Ag nanowires ClearOhm Ink-N (Cambrios Technologies Corp.) and spun at 3000 rpm for 30 s followed by a 1.5 min bake at 50 °C and a 1.5 min bake at 150 °C. 200 nm of Ag was evaporated on the top surface through a shadow mask to form the bus bar and the sides of the polymer embedded array were removed with a razor blade. A Ga/In eutectic was scratched into the back side to form a back contact. Details on electrical measurements can be found in ref. [12,19] Image analysis software (ImageJ) was used to measure the contacted area, with the outer perimeter set as the point at which the photocurrent fell to 0. After on substrate measurement, the polymer embedded wire array was mechanically removed from the growth substrate with a razor blade and 200 nm of Au was evaporated on the back.

Supporting Information

Supporting Information is available from the Wiley Online Library or from the author.

Acknowledgements

We are grateful to all of our mentors and family for their help and support through the years. This material is based upon work supported in part by the National Science Foundation (NSF) and the Department of Energy (DOE) under NSF CA No. EEC-1041895 and in part by the DOE under grant DE-EE0005311. Any opinions, findings and conclusions or recommendations expressed in this material are those of the author(s) and do not necessarily reflect those of NSF or DOE. D.B.T-E. acknowledges the NSF for fellowship support.

Received: February 28, 2013
Revised: April 16, 2013
Published online: June 10, 2013

[1] L. Hu, H. S. Kim, J.-Y. Lee, P. Peumans, Y. Cui, *ACS Nano* **2010**, *4*, 2955.
[2] F. Xu, Y. Zhu, *Adv. Mater.* **2012**, *24*, 5117.
[3] P. Lee, J. Lee, H. Lee, J. Yeo, S. Hong, K. H. Nam, D. Lee, S. S. Lee, S. H. Ko, *Adv. Mater.* **2012**, *24*, 3326.
[4] D.-S. Leem, A. Edwards, M. Faist, J. Nelson, D. D. C. Bradley, J. C. de Mello, *Adv. Mater.* **2011**, *23*, 4371.
[5] Z. Yu, L. Li, Q. Zhang, W. Hu, Q. Pei, *Adv. Mater.* **2011**, *23*, 4453.
[6] C.-H. Kim, S.-H. Cha, S. C. Kim, M. Song, J. Lee, W. S. Shin, S.-J. Moon, J. H. Bahng, N. A. Kotov, S.-H. Jin, *ACS Nano* **2011**, *5*, 3319.
[7] C.-C. Chen, L. Dou, R. Zhu, C.-H. Chung, T.-B. Song, Y. B. Zheng, S. Hawks, G. Li, P. S. Weiss, Y. Yang, *ACS Nano* **2012**, *6*, 7185.
[8] L. Li, Z. Yu, W. Hu, C.-h. Chang, Q. Chen, Q. Pei, *Adv. Mater.* **2011**, *23*, 5563.
[9] C. Yang, H. Gu, W. Lin, M. M. Yuen, C. P. Wong, M. Xiong, B. Gao, *Adv. Mater.* **2011**, *23*, 3052.
[10] C.-H. Chung, T.-B. Song, B. Bob, R. Zhu, H.-S. Duan, Y. Yang, *Adv. Mater.* **2012**, *24*, 5499.
[11] J. Wallentin, N. Anttu, D. Asoli, M. Huffman, I. Åberg, M. H. Magnusson, G. Siefer, P. Fuss-Kailuweit, F. Dimroth, B. Witzigmann, H. Q. Xu, L. Samuelson, K. Deppert, M. T. Borgström, *Science* **2013**, *339*, 1057.
[12] M. C. Putnam, S. W. Boettcher, M. D. Kelzenberg, D. B. Turner-Evans, J. M. Spurgeon, E. L. Warren, R. M. Briggs, N. S. Lewis, H. A. Atwater, *Energy Environ. Sci.* **2010**, *3*, 1037.
[13] E. Garnett, P. D. Yang, *Nano Lett.* **2010**, *10*, 1082.
[14] G. Mariani, P.-S. Wong, A. M. Katzenmeyer, F. Léonard, J. Shapiro, D. L. Huffaker, *Nano Lett.* **2011**, *11*, 2490.
[15] L. Tsakalakos, J. Balch, J. Fronheiser, B. A. Korevaar, O. Sulima, J. Rand, *Appl. Phys. Lett.* **2007**, *91*, 233117.

[16] C. E. Kendrick, H. P. Yoon, Y. A. Yuwen, G. D. Barber, H. Shen, T. E. Mallouk, E. C. Dickey, T. S. Mayer, J. M. Redwing, *Appl. Phys. Lett.* **2010**,*97*, 143108.
[17] Z. Fan, H. Razavi, J.-w. Do, A. Moriwaki, O. Ergen, Y.-L. Chueh, P. W. Leu, J. C. Ho, T. Takahashi, L. A. Reichertz, S. Neale, K. Yu, M. Wu, J. W. Ager, A. Javey, *Nat. Mater.* **2009**, *8*, 648.
[18] M. D. Kelzenberg, S. W. Boettcher, J. A. Petykiewicz, D. B. Turner-Evans, M. C. Putnam, E. L. Warren, J. M. Spurgeon, R. M. Briggs, N. S. Lewis, H. A. Atwater, *Nat. Mater.* **2010**, *9*, 239.
[19] M. D. Kelzenberg, D. B. Turner-Evans, M. C. Putnam, S. W. Boettcher, R. M. Briggs, J. Y. Baek, N. S. Lewis, H. A. Atwater, *Energy Environ. Sci.* **2011**, *4*, 866.
[20] K. E. Plass, M. A. Filler, J. M. Spurgeon, B. M. Kayes, S. Maldonado, B. S. Brunschwig, H. A. Atwater, N. S. Lewis, *Adv. Mater.* **2009**, *21*, 325.
[21] E. C. Garnett, W. Cai, J. J. Cha, F. Mahmood, S. T. Connor, M. Greyson Christoforo, Y. Cui, M. D. McGehee, M. L. Brongersma, *Nat Mater* **2012**, *11*, 241.
[22] S. M. Sze, K. K. Ng, *Physics of Semiconductor Devices*, Wiley-Interscience, Hoboken, NJ, USA **2007**.